

1 **THREE INTEGRATED PROCESS SIMULATION USING ASPEN PLUS®: PINE**  
2 **GASIFICATION, SYNGAS CLEANING AND METHANOL SYNTHESIS**

3 M. Puig-Gamero, J. Argudo-Santamaria, J.L. Valverde, P. Sánchez, L. Sanchez-  
4 Silva\*

5 Department of Chemical Engineering, University of Castilla –La Mancha, Avda.  
6 Camilo José Cela 12, 13071 Ciudad Real, Spain

7 \*Corresponding author phone: +34 926 29 53 00 ext. 6307; fax: +34 926 29 52 56;

8 e-mail: [marialuz.sanchez@uclm.es](mailto:marialuz.sanchez@uclm.es)

9  
10 **Keywords:** Biomass, gasification, PSA, methanol, syngas, Aspen Plus® simulation

22 **Abstract**

23       The methanol synthesis from syngas obtained through pine biomass gasification  
24 was studied using Aspen Plus® simulation software. The gasification process was  
25 simulated using a thermodynamic equilibrium model which is based on the minimization  
26 of the Gibbs free energy of the system. A double chamber gasifier, which allows the  
27 separation of the gasification and combustion zones to obtain a high-quality gas, was  
28 considered. Furthermore, part of the char was burnt in the combustion chamber increasing  
29 the bed temperature and generating all the energy needed in the process. On the other  
30 hand, effect of the gasification temperature and the steam to biomass (S/B) mass ratio  
31 during the gasification process on the syngas composition, tar yield and methanol  
32 production were evaluated. In this sense, the H<sub>2</sub>/CO ratio was calculated to establish the  
33 best operating conditions for the production of methanol, being the best calculated  
34 operational condition of the process 900°C and a S/B mass ratio of 0.9. In order to clean  
35 the syngas for the methanol synthesis and capture the greenhouse gases, a pressure swing  
36 adsorption (PSA) process was considered. Furthermore, the influence of pressure and  
37 temperature on the methanol synthesis was researched to select the optimal conditions for  
38 methanol production. Finally, the methanol synthesis waste stream was recycled to the  
39 combustion chamber in order to analyse its effect on the process performance.

40

41 **1. Introduction**

42       The current environmental problem due to the massive use of fossil fuel for power  
43 generation, has forced the search of new and more sustainable alternatives as renewable  
44 energy and new agreements to face the continuous energy demand. For this reason,  
45 several countries agreed at the Paris Climate Change Conference (COP21) to limit the  
46 global temperature increase in less than 2°C compared to that the beginning of the

47 industrial revolution by the year 2035 [1]. In this sense, the biomass is presented as one  
48 of the promising choice for the replacement of conventional fossil fuels in the near future,  
49 contributing to the reduction of greenhouse emissions. In addition, one of the main  
50 competitive advantage of biomass with respect to the rest of renewable energy is that it  
51 can obtain added value products similar to those obtained with fossil fuels and power.  
52 However, at the present, the technologies required for biomass transformation are not  
53 mature enough.

54 Lignocellulosic biomass can be converted to chemical products and biofuels via  
55 thermochemical or biochemical routes. However, the last one is a more expensive and  
56 complex technique than thermochemical route [2]. Pyrolysis, gasification, combustion  
57 and liquefaction are the most common thermochemical processes to convert the  
58 lignocellulosic biomass to biofuels. Among them, the gasification is considered as most  
59 cost-effective and efficient for lignocellulosic biomass conversion [2]. Moreover, the  
60 gasification is more environmentally friendly due to the low-oxidation conditions,  
61 emitting less greenhouse gases [3]. Biomass gasification can be defined as the conversion  
62 of biomass into a gaseous fuel in a partial oxidation atmosphere at high temperatures. The  
63 main gas product obtain is the syngas, which can be burnt directly, used as fuel for gas  
64 turbine, or can be used to produce added value chemicals. The gasifying agent used on  
65 gasification can be air, steam, oxygen or carbon dioxide. Air is currently the most used  
66 because of its low cost, but the syngas obtained has low heating value. Pure oxygen  
67 produce higher quality syngas but it involves high operating costs. For its part, steam  
68 gasification improves the quality of the product gas, increasing the hydrogen yield and  
69 decreasing the tar and char yield [4]. The syngas from biomass mainly consists of hydrogen  
70 and carbon monoxide but it also have methane, carbon dioxide, water vapor, nitrogen and  
71 some impurities like tars, ammonia and hydrogen sulphide.

72 One of the main technical barriers and problems for synthesis gas production is the  
73 presence of tars in the syngas. Among all chemical and physical techniques, catalytic  
74 conversion is the most used technique since the presence of catalyst can remove tar more  
75 effectively and, at the same time, convert tar into useful gas at lower temperature than  
76 non-catalytic gas tar conversion route [5] [6]. Dolomite, for its part, is presented as an  
77 attractive option since it is a cheap material and exhibits catalytic activity and  
78 effectiveness to reduce tars during gasification process in both laboratory and pilot scales  
79 [7, 8].

80 The syngas obtained from biomass gasification can be used for the synthesis of  
81 chemicals such as methanol. Methanol is an important industrial chemical, which can be  
82 used directly as a clean fuel or can be mixed with others conventional fuels. Furthermore,  
83 many chemical products such as formaldehyde, methyl tertiary butyl ether, acetic acid or  
84 gasoline can be obtained from it. The syngas obtained from biomass gasification must be  
85 cleaned before methanol synthesis. The most frequently used technology for CO<sub>2</sub> removal  
86 from syngas is the absorption process with MEA. However, this process is expensive and  
87 largescale is only cost-effective [9]. In this way, pressure swing adsorption (PSA) has  
88 become very prominent in the purification of gases for multiple applications. This  
89 technology reduces energy consumption without the need of using toxic and corrosive  
90 chemicals as in chemical absorption [10]. Several process to separate H<sub>2</sub> and CO by PSA  
91 system have been patented. Krishnamurthy et al. [11] studied a method to separate both  
92 components using two PSA systems. Recently, Batdorf et al. [12] proposed a method to  
93 remove CO<sub>2</sub> from effluent gas through the PSA, generating a syngas stream acceptable  
94 to produce methanol or other liquid fuels.

95 On the other hand, the process simulation is an increasingly important tool for the  
96 chemical industry that allows to scale up a process which requires a knowledge of the

97 influence of the operating conditions on the plant performance. In addition, the process  
98 simulation also allow to reduce costs and time [13]. There are many commercial  
99 simulators of chemical engineering processes, being Aspen Plus® one of the most used.

100 Although there are several studies about coal gasification simulation, nowadays,  
101 more and more researches are focused on the biomass gasification. Pauls et al., simulated  
102 the gasification of pine sawdust in the presence of both air and steam. They used a  
103 Bubbling Fluidized Bed gasifier including a temperature-dependent pyrolysis model and  
104 the inclusion of tar formation and reaction kinetics [14]. In addition, Zhai et al., proposed  
105 also a two-stage biomass pyrolysis and gasification scheme for pine sawdust. In this case,  
106 part of the gas product combusts in a burner outside of the gasifier to produce the flue gas  
107 and the heat required for pyrolysis and steam gasification. They established a zero-  
108 dimensional thermodynamic equilibrium model [15]. On the other hand, Nilsson et al.,  
109 simulated also a fluidized bed dividing it into three zones: pyrolysis of biomass,  
110 homogeneous and heterogeneous reactions, each one with its corresponding kinetics  
111 obtained from literature and experiments[16]. Finally, Im-orb et al., separated the  
112 gasification model into two sections, the first one combined pyrolysis and oxidation  
113 reactions which are assumed to be at thermodynamic equilibrium, and the second one,  
114 involved the char reduction reactions [17]. Fernández-López et al., simulated the  
115 gasification of an animal waste biomass in a dual gasifier. They used a model based on a  
116 Gibbs free energy reactor with the gasification and combustion zones separated [18].

117 Up to now, the most simulations using Aspen Plus® simulation software have focused  
118 on the gasification stage with different biomasses, temperatures and steam to biomass  
119 (S/B) mass ratio in order to improve the syngas composition. However, fewer studies  
120 have considered the tar formation and, thus, the addition of tar reforming using natural  
121 catalyst as a dolomite. Moreover, this study presents the novelty of simulating three

122 process integrated: the gasification process with tar reforming, the syngas cleaning using  
 123 PSA and the subsequent use for the methanol synthesis, becoming a product with a high-  
 124 added value. The present work includes the simulation of the biomass gasification, syngas  
 125 purification and its use in the methanol synthesis becoming a product with a high-added  
 126 value. In addition, the combination of different operating conditions, such as the  
 127 temperature and the S/B mass ratio in the gasification process were studied to establish the  
 128 best ones for the production of methanol. In this way, the best operating conditions  
 129 (temperature and pressure) in the case of methanol synthesis were also evaluated. Finally,  
 130 a recycle stream was considered in order to improve the system.

## 131 2. Materials and methods

### 132 2.1 Biomass sample

133 The biomass selected was a pine sample from the region of Castilla-La Mancha  
 134 (Spain). The Table 1 shows the ultimate and proximate analysis of the pine sample.

135 **Table 1.** Proximate and ultimate analysis of pine biomass.

<i>Ultimate Analysis (wt. %)*</i>					<i>Proximate Analysis (wt. %)<sup>*daf</sup></i>			
<i>C</i>	<i>H</i>	<i>N</i>	<i>S</i>	<i>O<sup>*diff</sup></i>	<i>Ash</i>	<i>VM<sup>*</sup></i>	<i>FC<sup>*diff</sup></i>	<i>Moisture</i>
52.7	5.52	0.01	0.08	41.7	2.7	61.6	31.3	4.4

136 <sup>\*daf</sup>: dry and ash free basis; <sup>O<sup>\*diff</sup></sup>: % of oxygen calculated from difference of C, H, N and S;  
 137 <sup>VM<sup>\*</sup></sup>: Volatile matter; <sup>FC<sup>\*diff</sup></sup>: % of fixed carbon calculated from the difference from moisture,  
 138 ash and volatile matter.

### 139 2.2 Aspen plus modelling

140 Figure 1 shows the Aspen Plus<sup>®</sup> flowsheet for the methanol synthesis from biomass.  
 141 The steps involved in the production of methanol from biomass are: gasification process,

142 syngas cleaning and methanol synthesis. In order to simplify the explanation of the  
143 simulation, the three main parts will be explained step by step. Firstly, the biomass is  
144 gasified using steam as gasifying agent. The product gas is fed to PSA system in which  
145 the gas is cleaning and adjusting to achieve a H<sub>2</sub>/CO ratio close to 2.4-2.5. Finally, the  
146 syngas with the correct ratio is fed to methanol synthesis.

147 In the simulation, the biomass is defined as non-conventional component, specifying  
148 its ULTANAL and PROXANAL analysis. The HCOALGEN and DCOALGEN models  
149 were selected for the enthalpy and density of the solids calculation, respectively. The ash  
150 was selected as non-conventional component and 100% of ash was fixed for the ultimate  
151 and proximate analysis. The fluid-dynamic package selected was Peng-Robinson with  
152 Boston Mathias function, being the appropriate for high temperature gasification  
153 processes [19]. The char (it was considered to be 100 % carbon) and catalyst (Dolomite  
154 and Cu/ZnO) were defined as conventional solid, whereas the rest of the components: H<sub>2</sub>,  
155 CO, CO<sub>2</sub>, CH<sub>4</sub>, H<sub>2</sub>O, H<sub>2</sub>S, N<sub>2</sub>, NH<sub>3</sub>, C<sub>6</sub>H<sub>6</sub> and CH<sub>3</sub>OH, were defined as fluids.

### 156 2.2.1 Gasification process

157 In this work, an equilibrium model based on a Gibbs free energy minimization was  
158 used to model a dual fluidized bed gasifier for the conversion of pine biomass into syngas.  
159 In this kind of reactors, the combustion zone is independent of the gasification zone,  
160 moreover, the combustion heat is used in the rest of the process, involving energy savings.  
161 On the other hand, a catalyst bed of dolomite was used to reduce the tar obtained in the  
162 product gas. Figure 2 shows the Aspen Plus<sup>®</sup> flowsheet of the gasification process and  
163 Table 2 lists a brief explanation of the blocks used.

164 The main assumption considered in this part of the process are the following [19, 20]:

- 165 1. Biomass feed rate is 100 kg/h.
- 166 2. Process was steady state and isothermal.
- 167 3. Char only contained carbon and ash.
- 168 4. Ash is considered to be inert
- 169 5. Pressure and temperature were uniform inside the gasifier.
- 170 6. No heat and pressure losses took place in the gasifier.
- 171 7. All gases were ideal.
- 172 8. No unconverted carbon was present in the product.
- 173 9. Drying and pyrolysis processes were instantaneous.
- 174 10. Tar composition was assumed to be  $C_6H_6$ .

175 Stream 1, whose composition was the biomass, was fed under ambient conditions (25°C  
176 and 1 atm) to the block R-1 to simulate an instant drying and pyrolysis process. In this  
177 process, biomass was separated into its constituent components and ash, the yields  
178 distribution, which determined the each component mass flow that left the block R-1, was  
179 specified according to the elemental analysis of the biomass feedstock. Subsequently, the  
180 char combustion process was carried out in block R-5 to achieve the gasification  
181 temperature, decreasing the gasifier energy requirement. The gasification zone and  
182 combustion zone temperature was the same because it was considered homogenous over  
183 the whole process. The amount of char for combustion process was calculated by the  
184 design specification DS-4, (Table A4) and was split in the separator column SEP-1.  
185 Furthermore, the air flow was calculated using a design specification (DS-3, Table A3)  
186 and taking into account an air excess of 1.2 regarding the char burnt in the combustion  
187 chamber.



188

189

190

191

192

193

194

195

196

197

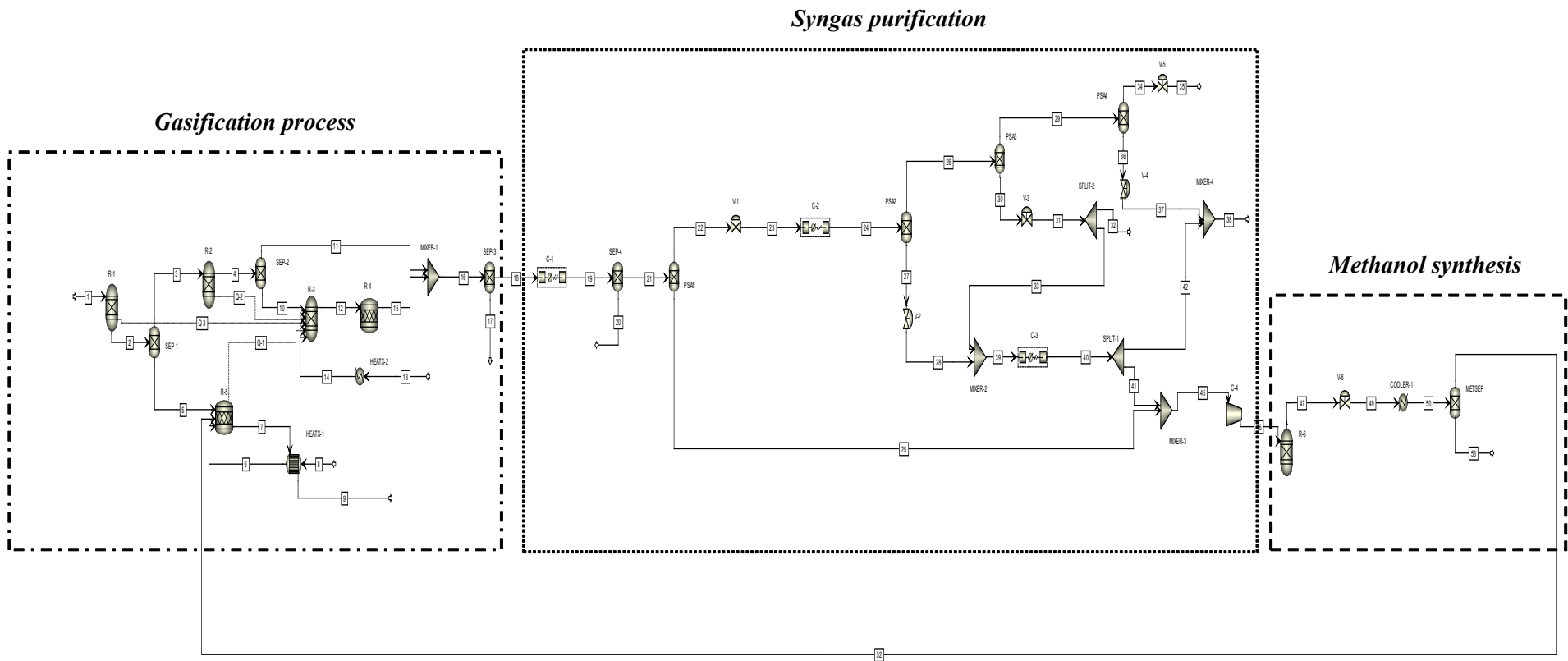
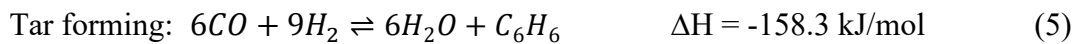
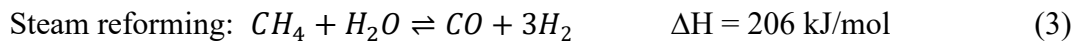
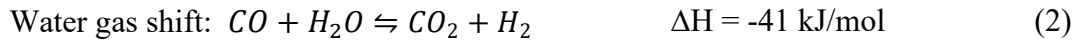


Figure 1. Aspen Plus® flowsheet process

198 Stream 3 containing O<sub>2</sub>, H<sub>2</sub>, H<sub>2</sub>O, C, S and N<sub>2</sub> entered to the equilibrium reactor R-  
 199 2. In this reactor, C, H<sub>2</sub>, CO<sub>2</sub>, CO, CH<sub>4</sub>, H<sub>2</sub>S and NH<sub>3</sub> were fixed as the main reaction  
 200 products. The outlet gas was introduced into a new separator column where H<sub>2</sub>S and NH<sub>3</sub>  
 201 (stream 11) were split from the main fuel stream consisting of C, H<sub>2</sub>, CO<sub>2</sub>, CO and CH<sub>4</sub>  
 202 (stream 10). Then, the last one was directed to the block R-3 where the gasification  
 203 process took place. The gasifying agent steam was added to the reactor R-3 as steam at 1  
 204 bar and 150 °C (stream 14). Moreover, the energy stream Q-1 simulated the energy which  
 205 was transferred from the combustion chamber to the gasification one. In addition, blocks  
 206 R-1 and R-2 were also energy integrated with the gasification block R-3 by the energy  
 207 streams Q-3 and Q-2, respectively. The reactions involved in gasification process are  
 208 summarized below:

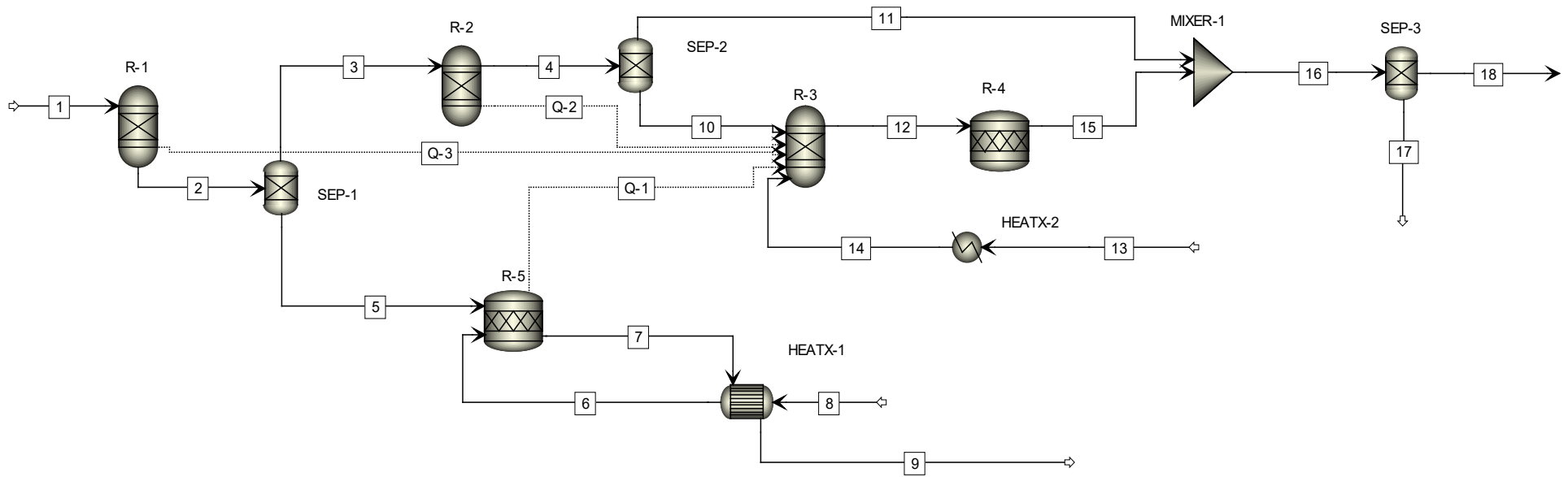


209 On the other hand, the tar reforming using dolomite as a catalyst was simulated in the  
 210 block R-4. The aim of this block was to convert the tar to syngas due to the tar could condense  
 211 downstream, blocking the pipelines and causing several problems in compressor or pumps.  
 212 The reactions involved in the tar decomposition with dolomite are the following:

213

214

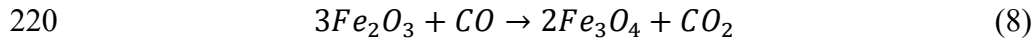
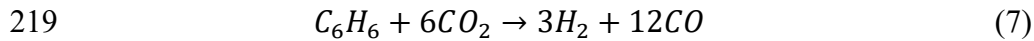
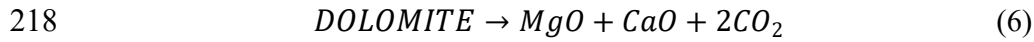
215



216

217

**Figure 2.** Aspen Plus® flowsheet simulation of the gasification process.



221 Finally, the gas product of gasification process (stream 16) was fed to block SEP-3  
 222 to separate the active char (stream 17) from the rest of syngas compounds.

223 2.2.2 Syngas cleaning: Pressure swing adsorption (PSA)

224 The aim of this part was to cleaning the outlet gas of gasification in order to obtain a  
 225 high quality syngas which will be used for the methanol synthesis. The syngas for  
 226 methanol synthesis must satisfy the following specification:

227 
$$\bullet \frac{H_2 - CO_2}{CO + CO_2} \approx 2.1 \quad (9)$$

228 
$$\bullet \frac{H_2}{CO} = 2.4 - 2.5 \quad (10)$$

229 
$$\bullet \frac{CO_2}{CO} = 0.13 - 0.14 \quad (11)$$

230 A pressure swing adsorption was simulated to clean the syngas and obtain de optimal  
 231 ratio required. The outlet gas of gasification was introduced into the PSA system, which  
 232 consisted of four units, as shown in Figure 3. All of them were simulated in a simplified  
 233 way, by ideal separators, but working at realistic temperature and pressure (35 °C and 30  
 234 atm, respectively) [21].

235 The syngas obtained from gasification process (stream 18) was compressed to 30 atm  
 236 and cooled down to 35°C by the multistage compressor C-1. Then, stream 19 was fed to  
 237 the column separator SEP-4 to separate the condensed water from the gas stream 21 that  
 238 went to the PSA system. The PSA system was able to achieve a pure syngas stream to

239 adjust the stoichiometric ratio of methanol feed and, simultaneously, capture CO<sub>2</sub> and  
 240 CH<sub>4</sub> for their subsequent sequestration.

241 **Table 2.** Blocks description used in the gasification model.

<i>NAME</i>	<i>TYPE</i>	<i>DESCRIPTION</i>
<i>R-1</i>	RYIELD	Biomass pyrolysis reactor, it decomposed the biomass into its compounds and ash. It operated at 1 atm and 800, 900 or 1000°C depending on the simulation.
<i>SEP-1</i>	SEP	Separator of the amount of char necessary to achieve the gasification temperature.
<i>R-2</i>	RGIBBS	It models chemical equilibrium minimizing the Gibbs free energy. It was used to produce CO <sub>2</sub> , CO, CH <sub>4</sub> , H <sub>2</sub> S and NH <sub>3</sub> . It operated at 1 atm and 800, 900 or 1000°C depending on the simulation.
<i>SEP-2</i>	SEP	Separator of H <sub>2</sub> S and NH <sub>3</sub> from C, H <sub>2</sub> , CO <sub>2</sub> , CO and CH <sub>4</sub> .
<i>R-3</i>	RGIBBS	Gasifier. It operated at 1 atm and 800, 900 or 1000°C depending on the simulation.
<i>R-4</i>	RSTOIC	This reactor allows to introduce a catalyst. It was used to model the tar reforming using Dolomite as a catalyst. It operated at 1 atm and 800, 900 or 1000°C depending on the simulation.
<i>SEP-3</i>	SEP	It separated the active coal from the syngas.
<i>R-5</i>	RSTOIC	Char combustion reactor. It operated at 1 atm and 800, 900 or 1000°C depending on the simulation.
<i>HEATX-1</i>	HEATX	Exchange heat between the outlet stream from R-5 and the air inlet stream which was warmed up to 150°C
<i>HEATX-2</i>	HEATER	Heater to warm up the gasifying agent (water steam) to 150°C.

242

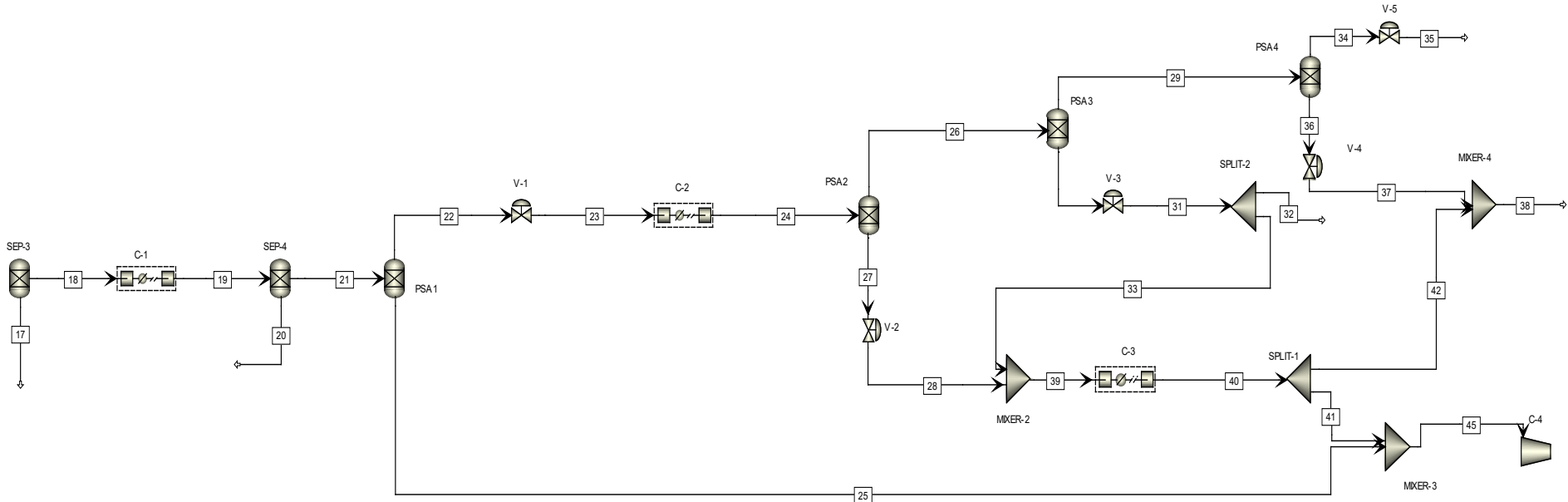
243 In the first PSA unit, high purity H<sub>2</sub> was separated (stream 25). There was no pressure  
244 drop inside the block. The first PSA unit was depressurized to regenerate the adsorbent.  
245 Every depressurization have been simulated by a valve located at the PSA off-gas stream.  
246 Then, top stream 23 was again compressed to 30 atm in the compressor C-2 before  
247 entering into the second PSA unit (PSA2). In this step, CO was separated as the adsorbed  
248 component (stream 27), recovered in the depressurization. Top PSA-2 stream 26 was  
249 introduced in the third PSA unit (PSA3) where CH<sub>4</sub> and CO<sub>2</sub> were split in streams CH<sub>4</sub>-  
250 rich top (29) and CO<sub>2</sub>-rich bottom (30). On the one hand, top stream 29 entered to the last  
251 PSA unit (PSA4) for the CH<sub>4</sub> capture. On the other hand, a fraction of the bottom gas  
252 formed by rich CO<sub>2</sub> was mixed with the rich-CO stream 28 coming from the second PSA  
253 unit.

254 Then, stream 39, whose composition was the mixture of CO and CO<sub>2</sub>, was  
255 compressed up to 30 atm and mixed with the rich H<sub>2</sub> stream (25) to adjust the  
256 specifications 9, 10 and 11. This adjustment was carried out by the design specifications  
257 DS-1 and DS-2 (Table A1 and A2). Finally, Table 3 and 4 show a brief explanation of  
258 the blocks used in the syngas cleaning and the percentage considered of component  
259 recovery in the PSA system according to F.J. Gutiérrez Ortiz et al., [9], respectively.

### 260 2.2.3 Methanol synthesis process

261 Once the syngas was purified and the specifications were achieved, the pure syngas  
262 stream was introduced to methanol synthesis reactor. The blocks used to simulate the  
263 methanol shyntesis are summarized in Table 5 and Figure 4 shows the methanol synthesis  
264 flowsheet. The standard operation condition of the methanol synthesis are in the ranges  
265 of 50 to 100 atm and 220 to 280 °C [9]. In this work, the pressure and temperature of  
266 methanol synthesis were varied and evaluated.

267



268

**Figure 3.** Aspen Plus® flowsheet simulation of the syngas cleaning.

269

270

271

**Table 3.** Blocks description used in the syngas cleaning model.

<i>NAME</i>	<i>TYPE</i>	<i>DESCRIPTION</i>
<i>C-1, C-2 and C-3</i>	MULTISTAGE COMPRESSORS	The multistage compressors were used to compress to 30 atm and cool down to 35°C the unclean gas, the PSA2 inlet stream and the CO and CO <sub>2</sub> mixture, respectively.
<i>SEP-4</i>	SEP	Separator of the water condensed and the syngas.
<i>PSA1, PSA2, PSA3 and PSA4</i>	SEP	Separator to adsorb and separate at 30 and 35 atm rich H <sub>2</sub> , rich CO, rich CO <sub>2</sub> and rich CH <sub>4</sub> , respectively.

272

273

**Table 4.** Percentage of component recovered in the PSA system [9].

	<i>PSA-1 (top)</i>	<i>PSA-2 (bottom)</i>	<i>PSA-3 (top)</i>	<i>PSA-3 (bottom)</i>	<i>PSA-4 (top)</i>
<i>H<sub>2</sub></i>	95	-	4.5	0.5	-
<i>CO</i>	-	98	1.5	0.5	-
<i>CO<sub>2</sub></i>	-	1	9	90	-
<i>CH<sub>4</sub></i>	-	1	90	9	100
	<i>Rich H<sub>2</sub> stream (25)</i>	<i>Rich CO stream (27)</i>	<i>CH<sub>4</sub> stream (29)</i>	<i>Rich CO<sub>2</sub> stream (31)</i>	<i>Rich CH<sub>4</sub> stream (35)</i>

274

275

First, the pure syngas stream was compressed and heated up to the operating pressure

276

and temperature. Then, the stream was introduced in the reactor R-6 to accomplish the

277

methanol production. The catalyst selected to the synthesis was Cu/ZnO due to be one of

278

the most commercially-available catalyst for methanol production. The following

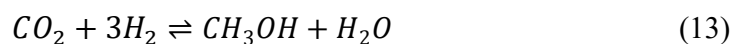
279

reactions were involved during the synthesis:

280



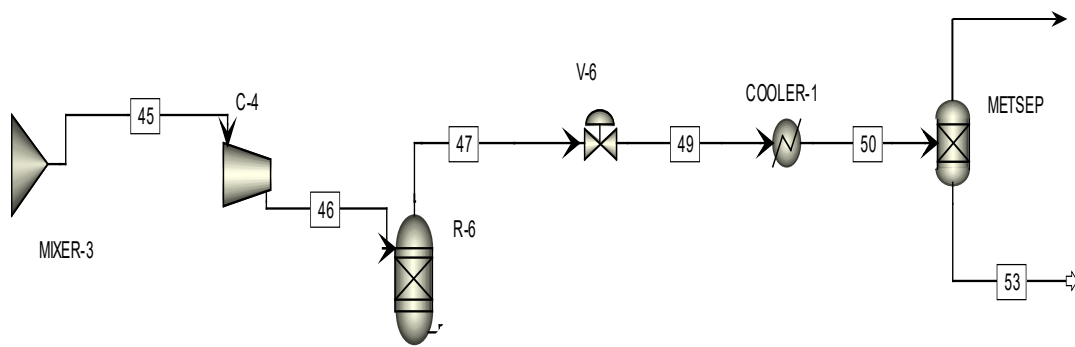
281





282 The conversions were 35% and 17 % for CO and CO<sub>2</sub>, respectively [22]. Then,  
 283 reaction product was depressurized to 1 atm and cooled down to 25°C to condense and  
 284 separate the crude methanol from the gas-phase in the METSEP flash, getting by the  
 285 bottom pure methanol as the final product. Finally, top stream 52, which contained  
 286 unconverted H<sub>2</sub>, was recycled to the combustion chamber to reduce the amount of char  
 287 necessary to reach the gasification temperature.

288



289 **Figure 4.** Aspen Plus® flowsheet simulation of methanol synthesis.

290

291 **Table 5.** Blocks description used in the methanol synthesis.

<i>NAME</i>	<i>TYPE</i>	<i>DESCRIPTION</i>
<b><i>C-4</i></b>	COMPRESSOR	It was used to compress and to purify the syngas.
<b><i>R-6</i></b>	REQUIL	Methanol synthesis reactor.
<b><i>COOLER-1</i></b>	COOLER	It was used to cool down to 25°C the methanol produced to separate it.
<b><i>METSEP</i></b>	SEP	Separator of the crude methanol and gas-phase and impurities.

292

293 **3. Results and discussion**

294 3.1 Gasification simulation model

295 3.1.1 Model validation

296 The double chamber gasifier pilot-plant of the British Columbia University [20] was  
 297 considered to validate the present gasification model and check its accuracy. For that  
 298 purpose, a comparison between the predicted and experimental gas composition was  
 299 made. This plant was selected due the biomass used was softwood pellet, whose  
 300 composition (Table 6) was similar to the used in this study (Table 1). The gasifier operates  
 301 at 831°C and atmospheric pressure, the gasifying agent used is steam and the steam to  
 302 biomass mass flow ratio is 0.2.

303 **Table 6.** Proximate and ultimate analysis of softwood biomass.

<i>Ultimate Analysis (wt.%)<sup>*</sup></i>					<i>Proximate Analysis (wt.%)<sup>*daf</sup></i>			
<i>C</i>	<i>H</i>	<i>N</i>	<i>S</i>	<i>O<sup>*diff</sup></i>	<i>Ash</i>	<i>VM<sup>*</sup></i>	<i>FC<sup>*diff</sup></i>	<i>Moisture</i>
50.8	6.26	0.22	0.10	41.6	1	81.7	17.3	5.4

304 <sup>\*daf</sup>: dry and ash free basis; <sup>O<sup>\*diff</sup></sup>: % of oxygen calculated from difference of C, H, N and S;  
 305 <sup>VM<sup>\*</sup></sup>: Volatile matter; <sup>FC<sup>\*diff</sup></sup>: % of fixed carbon calculated from difference from moisture, ash  
 306 and volatile matter.

307 Table 7 compares the syngas composition between the present model and the  
 308 experimental data both obtained using the same operating conditions: gasification  
 309 temperature of 831°C, atmospheric pressure and steam as gasifying agent.

310

311 **Table 7.** Comparison between the syngas composition (vol.% dry basis) obtained with  
 312 the simulation model and experimental data.

<i>Compound</i>	<i>Experimental composition (vol.% db)</i>	<i>Predicted composition (vol.% db)</i>
-----------------	--	---

$H_2$	45-55	57
$CO$	21-25	20
$CO_2$	18-22	18
$CH_4$	2-4	2.2

313 Db: dry bases

314 The results obtained from the simulation were in good agreement with the  
 315 experimental ones. Main differences could be attributed to the use of an equilibrium  
 316 model in the proposed simulation while the experimental data took into account the  
 317 reaction kinetics being these results more rigorous. The error obtained were only 5% and  
 318 7% for the  $H_2$  and  $CO$ , being acceptable error. Therefore, the simulation can be considered  
 319 valid to reproduce a gasification process.

320

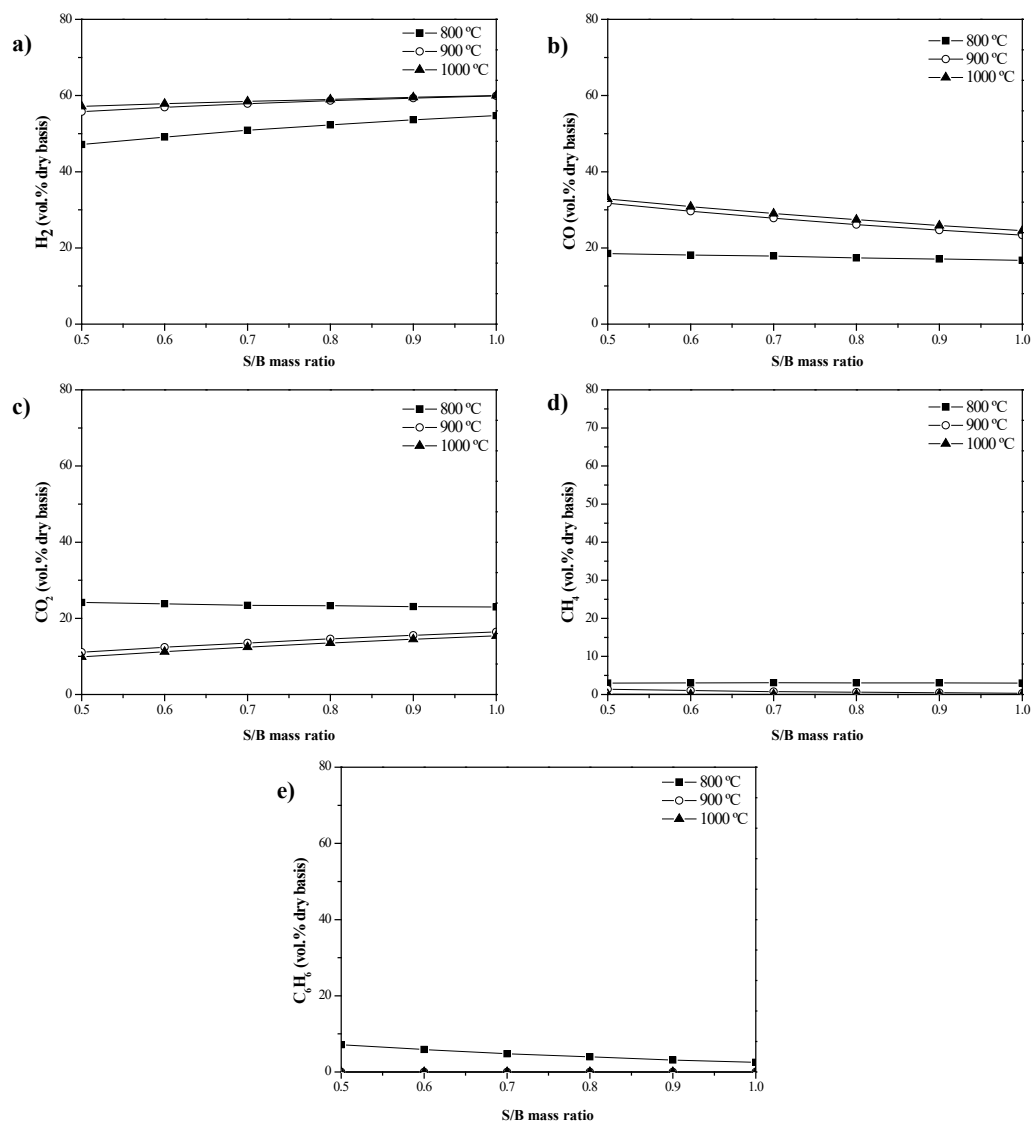
### 321 3.1.2 Sensitivity analysis

322 In this section, the effect of the operating conditions (temperature and steam to biomass  
 323 mass ratio) on syngas composition, tar conversion and methanol production are discussed.  
 324 In order to evaluate these processes, the simulation was carried out based on a simple  
 325 assumption. One of these parameters was varied while the rest of them were kept constant.  
 326 In this sense, the gasification temperature was varied between 800 and 1000°C and the  
 327 S/B mass ratio between 0.5 and 1 according to Shen et al. and Pala et al.[19, 23]. In  
 328 addition, the feed rate was fixed at 100 kg/h for all cases.

#### 329 3.1.2.1 Effect of steam to biomass (S/B) mass flow ratio

330 Figure 5 shows the effect of the S/B ratio on the main gases evolved ( $H_2$ ,  $CO$ ,  $CO_2$ ,  
 331  $CH_4$ , and  $C_6H_6$ ) during pine gasification at the three gasification temperatures studied  
 332 (800, 900 and 1000 °C). It can be observed that the S/B mass ratio had a weak effect on

333 the gas composition, especially when the S/B ratio achieved a value of 0.75. H<sub>2</sub> and CO<sub>2</sub>  
334 yield increased when the S/B mass ratio also increase whereas the CO and CH<sub>4</sub>  
335 production decreased with S/B mass ratio. These results are in good agreement with other  
336 authors (Fernandez-Lopez et al., and Pala et al., [18, 19]). This fact was explained by the  
337 water gas (Reaction 1), water gas-shift (Reaction 2) and steam reforming of methane  
338 (Reaction 3) reactions which were favoured at high steam flow. Thus, and accordingly to  
339 Le Chatelier's principle, the higher the steam flow the higher the CO, CO<sub>2</sub> and H<sub>2</sub> yields  
340 observed. However, the CO concentration decreased with increasing S/B ratio. This is  
341 due to CO reacting with steam in water gas shift reaction, increasing H<sub>2</sub> and CO<sub>2</sub>  
342 concentrations. In the case of CH<sub>4</sub>, its production decreased with higher steam flow due  
343 to it reacting with steam in the reforming of methane. Even then, it kept practically the  
344 same production in all cases.



345

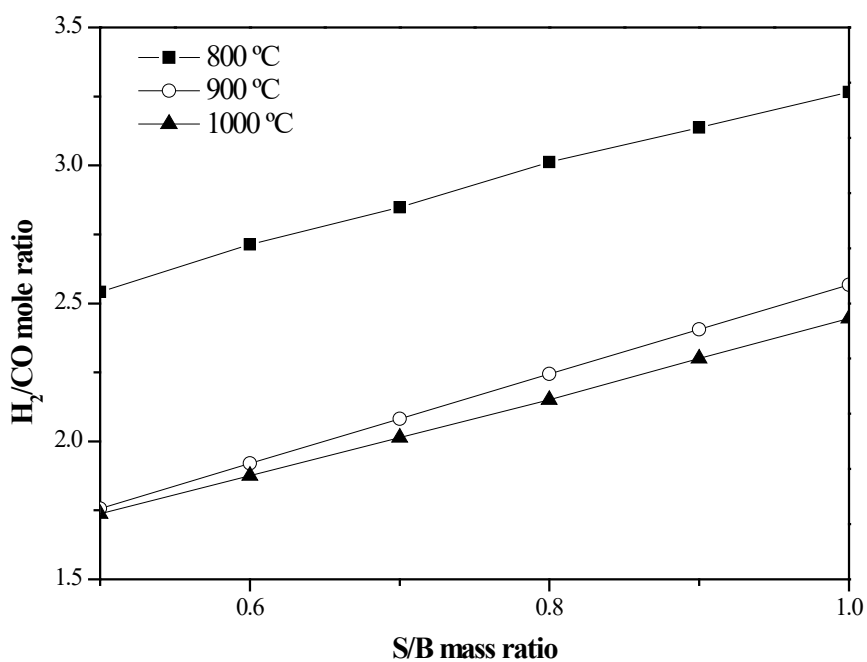
346 **Figure 5.** Effect of the S/B mass ratio on the syngas composition (dry basis) a) H<sub>2</sub>; b)  
 347 CO; c) CO<sub>2</sub>; d) CH<sub>4</sub>; e) C<sub>6</sub>H<sub>6</sub> at three gasification temperatures studied.

348 Regarding tar production, the CO reacting with H<sub>2</sub> to obtain H<sub>2</sub>O and C<sub>6</sub>H<sub>6</sub>. Thus, an  
 349 increase in the S/B mass ratio favoured backward the reaction decreasing tar formation.  
 350 Nevertheless, the quantity of tar produced was low, being practically constant especially  
 351 at higher temperatures.

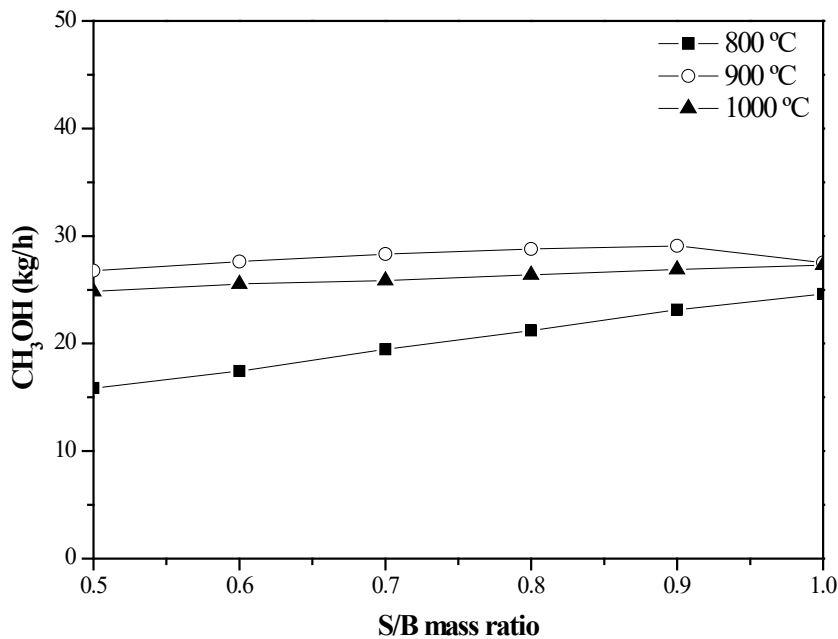
352 Figure 6 shows the S/B mass ratio effect on the H<sub>2</sub>/CO mole ratio in the product gas  
 353 composition at the three temperatures studied. It was observed that the H<sub>2</sub>/CO ratio

354 increased with the S/B mass ratio. The main reason was the effect of Water gas shift  
355 reaction due to it favoured hydrogen formation accompanied with CO concentration  
356 reduction. It is really important to take into account this ratio if the syngas is going to be  
357 used in a process to produce high added-value products such as Fischer-Tropsch or  
358 methanol synthesis. To use the syngas in the methanol production, the H<sub>2</sub>/CO ratio should  
359 be 2.4, which was achieving with 0.9 of S/B mass ratio at 900°C.

360 Finally, the influence of S/B mass ratio on the methanol production was presented in  
361 Figure 7. The higher the S/B ratio, the higher the methanol production was. However, a  
362 maximum was observed at 900 °C with S/B mass ratio of 0.9. This fact could be attributed  
363 that H<sub>2</sub>/CO molar ratio obtained at this operating conditions was 2.4, which is needed for  
364 the methanol synthesis.



365  
366 **Figure 6.** Effect of the S/B mass ratio on H<sub>2</sub>/CO mole ratio at three temperatures  
367 studied.



368

369 **Figure 7.** Effect of the S/B mass ratio on the CH<sub>3</sub>OH composition (kg/h) at different  
 370 temperatures.

371 *3.1.2.2 Effect of gasification temperature*

372 The gasification temperature is also a key parameter to optimize the hydrogen  
 373 production. In the proposed model, three temperatures were studied to simulate the  
 374 gasification: 800, 900 and 1000°C. It was observed that H<sub>2</sub> and CO concentrations  
 375 increased with increase in temperature whereas CO<sub>2</sub> and CH<sub>4</sub> concentrations were  
 376 favoured at low temperatures (Figure 5). Similar trends were observed by Shen et  
 377 al.,(2008) and Pala et al.,(2017) [19, 23]. The Boudouard reaction, water gas and steam  
 378 reforming of methane are endothermic reactions. In this type of reactions (endothermic  
 379 reactions) and accordingly to Le Chatelier's principle, an increase in the gasification  
 380 temperature led to an increase in the products production [18]. Therefore, higher  
 381 temperatures favour the CO and H<sub>2</sub> production, decreasing the CO<sub>2</sub> and CH<sub>4</sub> amounts in  
 382 the resulted syngas. For its part, the water gas shift is an exothermic reaction, thus, it is

383 favoured at low temperatures. Therefore, it led to an increase of H<sub>2</sub> and CO concentration  
384 with the temperature. On the other hand, water gas shift reaction is an exothermic  
385 reaction, being favoured at low temperatures. Higher temperatures favoured its backward  
386 reaction. For this reason, the higher the temperature, the higher the CO production and  
387 the lower the CO<sub>2</sub> yield was. Regarding to C<sub>6</sub>H<sub>6</sub> production, it can be observed the tar  
388 production was higher when the gasification temperature increased. This fact is due to the  
389 tar formation exothermic reaction was favoured at low temperatures [7].

390 Relating to H<sub>2</sub>/CO molar ratio, Figure 6 shows the effect of the gasification  
391 temperature on the H<sub>2</sub>/CO molar ratio decreased when the temperature was higher. The  
392 reason was that the increasing CO production was higher than the increasing H<sub>2</sub>  
393 production indicating that the Boudouard reaction was the dominant reaction over the  
394 Water gas reaction for the gasification temperature range studied [4]. However, this  
395 difference was more prominent at lower temperatures, being H<sub>2</sub>/CO molar ratio similar  
396 between 900-1000 °C. On the other hand, the methanol production was favoured at high  
397 gasification temperatures (Figure 7) due to the H<sub>2</sub> and CO production was also favoured  
398 at high gasification temperatures. As aforementioned, it can be observed a maximum at  
399 900 °C with S/B mass ratio of 0.9.

400 Finally, Table 8 presents the results obtained of gas, tar and char yields at the S/B mass  
401 ratio of 0.6 for the three gasification temperatures studied.

402



403 **Table 8.** Gas, tar and char yield results at three gasification temperatures studied for  
 404 S/B mass ratio of 0.6.

<i>Temperature (°C)</i>	<i>Gas yield (wt. %)</i>	<i>Tar yield (wt. %)</i>	<i>Char yield (wt. %)</i>
<b>800</b>	85.90	12.36	1.84
<b>900</b>	98.18	$3.0 \cdot 10^{-3}$	1.74
<b>1000</b>	98.16	$4.4 \cdot 10^{-10}$	1.72

405  
 406 The results obtained were in a good agreement with effects above explained. The  
 407 higher the temperature, the higher the gas yield and the lower the tar and char yield were.  
 408 Similar trends were reported by Luo et al., [24]. The increasing gas yield could be  
 409 attributed to the greater production of gas in the initial pyrolysis at higher temperatures  
 410 due to the enhancement of the endothermic gasification reactions. However, the  
 411 difference between 900°C and 1000°C was negligible. Thus, a rise in gasification  
 412 temperature above the 900°C did not improve the process, but this rise could be increase  
 413 the operational cost significantly.

414 On the other hand, tar content decreased from 12.36% to almost zero. It could be said  
 415 that, at 900°C, tar content could be considered almost non-existent but it was really  
 416 important to take it into account owing to the operational problems caused.

417 Finally, the decreasing trend of char content with higher temperatures was caused by  
 418 the higher availability of carbon to be converted in CO and CO<sub>2</sub> through the Water gas  
 419 (Reaction 1) and Boudouard (Reaction 4) reactions, being favoured at high temperatures.

420

421 *3.1.2.3 Tar cracking*

422 One of the main technical barriers for the syngas production is the presence of tar  
423 coming from the gasification process. Tars can condensed on equipment at moderate  
424 temperatures causing some problems such as the block of filters, valves and tubes,  
425 material corrosion or catalyst deactivation. According to the simulation performed, tar  
426 production was hindered with increasing temperatures and steam flowrates. Dolomite was  
427 used as the catalyst in the decomposition of tar due to its low cost [7].

428 At 900°C and 1000°C, tar conversion was complete. Moreover, at these temperatures,  
429 tar formation was low and gas composition was not modified after the cracking. However,  
430 at 800°C tar conversion was not complete, its conversion was enhancing when the amount  
431 of steam flow was increasing. Table 9 displays the gas composition after the tar cracking  
432 at the different S/B mass ratio studied. Figure 8 shows the comparison between the  
433 product gas composition before and after tar cracking for the S/B mass ratio of 0.6 at 800  
434 °C. It can be observed that, in dry basis, H<sub>2</sub> and CO<sub>2</sub> composition decreased while CO  
435 increased and CH<sub>4</sub> kept almost constant. This trend was explained through tar cracking  
436 reactions (6, 7 and 8). CO<sub>2</sub> was produced in reaction 6 and 8 but its consumption in  
437 reaction 7 was higher. However, CO was highly produced in reaction 7. For its part, H<sub>2</sub>  
438 was produced by means of tar cracking reaction, thus its concentration should increase.  
439 However, a decrease in H<sub>2</sub> was observed in Figure 8 due to it is expressed in dry basis  
440 and water content also decreased after tar cracking.

441

442 **Table 9.** Gas product composition (%.vol dry basis) after tar cracking at 800°C for  
443 different S/B mass ratio.

---

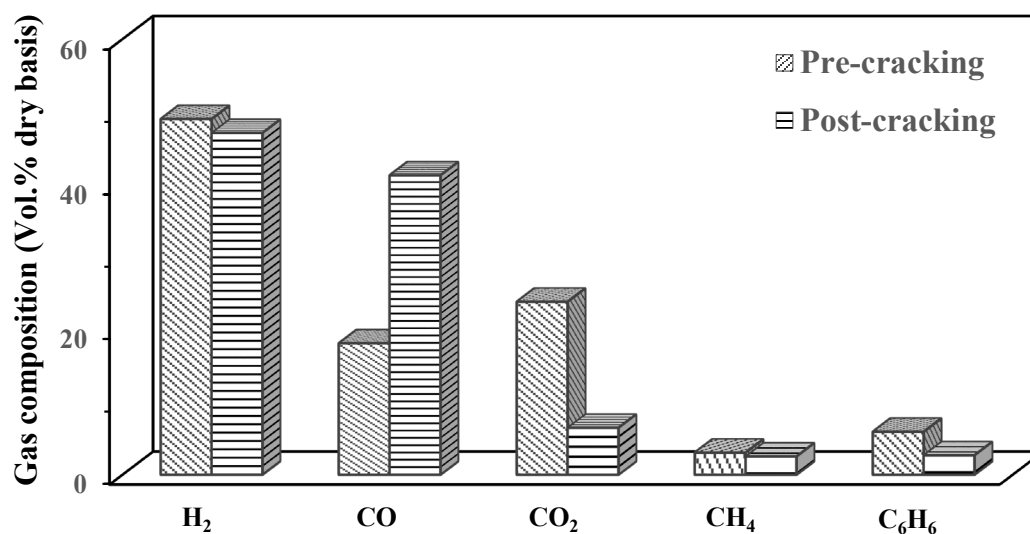
*S/B mass ratio*

---

	<i>0.5</i>	<i>0.6</i>	<i>0.7</i>	<i>0.8</i>	<i>0.9</i>	<i>1</i>
<i>Conversion (%)</i>	40	45	55	70	85	100
<i>H<sub>2</sub><sup>db</sup> (vol. %)</i>	45.36	47.08	48.58	49.61	50.78	51.84
<i>CO<sup>db</sup> (vol. %)</i>	43.02	41.24	40.74	41.43	40.58	39.25
<i>CO<sub>2</sub><sup>db</sup> (vol. %)</i>	5.68	6.47	6.36	5.47	5.75	6.43
<i>CH<sub>4</sub><sup>db</sup> (vol. %)</i>	2.46	2.52	2.56	2.51	2.50	2.47
<i>C<sub>6</sub>H<sub>6</sub><sup>db</sup> (vol. %)</i>	3.48	2.69	1.77	0.98	0.39	0.00

444 db: Dry basis

445



446 **Figure 8.** Gas composition (vol.% dry basis) before and after tar cracking at 800°C and  
447 S/B mass ratio of 0.6.

448 To sum up, the operational conditions selected for the gasification process were 900°C  
449 and a steam to biomass mass ratio of 0.9 because it is achieved the best results in syngas  
450 composition and methanol production. Although the process at 1000°C showed in general  
451 better results, they are closed to the results obtained at 900°C. Thus, trying to save energy

452 and costs, it was decided to simulate the process at 900°C. Moreover, the H<sub>2</sub>/CO molar  
453 ratio obtained at these conditions were 2.41, which was closed to the syngas specification  
454 needed for the methanol synthesis facilitating its syngas purification.

### 455 3.2 Methanol synthesis simulation

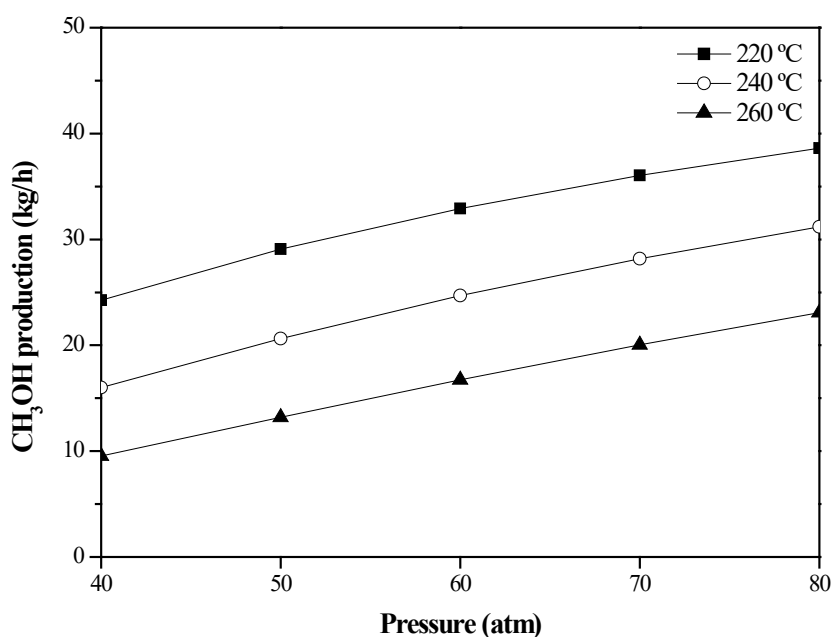
#### 456 3.2.1 Model validation

457 Methanol synthesis model was less complex than the gasification one. The bottleneck  
458 of this process was the low conversion achieved in reactions 12 and 13. In order to  
459 validate and check the accuracy of the reactor where the methanol synthesis took place,  
460 firstly, the process was simulated with a stoichiometric reactor, fixing the fractional  
461 conversions at 0.35 for CO in reaction 12 and 0.17 for CO<sub>2</sub> in reaction 13 using Cu/ZnO  
462 catalyst and operating conditions (240°C and 51 atm) both reported by Trop et al., (2014)  
463 [22] . Then, it was simulated with an equilibrium reactor fixing the pressure and  
464 temperature conditions. The results obtained were 16.5 and 15.4 kg/ h of methanol for  
465 stoichiometric reactor and equilibrium reactor, respectively. The error obtained was  
466 ±7.1%. Therefore, the model proposed could be considered as a valid model to simulate  
467 the methanol synthesis.

#### 468 3.2.2 Sensitivity analysis

469 In order to optimize the process, the pressure and temperature influence on the  
470 methanol production was evaluated. Different studies reported that typical operation  
471 conditions of the synthesis were in the ranges from 220 to 280 °C and 50 to 100 atm [21,  
472 22]. At higher temperatures, the catalyst could be damaged, producing its sintering and  
473 fusion. On the other hand, lower temperatures could reduce the reaction rate [21]. For this  
474 reason, the model proposed was simulated at standard temperatures and pressures ranges.  
475 Figure 9 shows the methanol production at different temperatures and pressures studies.

476 It was observed that the methanol yield was improved at high pressures and lower  
477 temperatures. Although the methanol production is favoured at high pressures, a pressure  
478 of 55 atm was selected in order to avoid operational issues observed at higher pressures  
479 [19, 21].

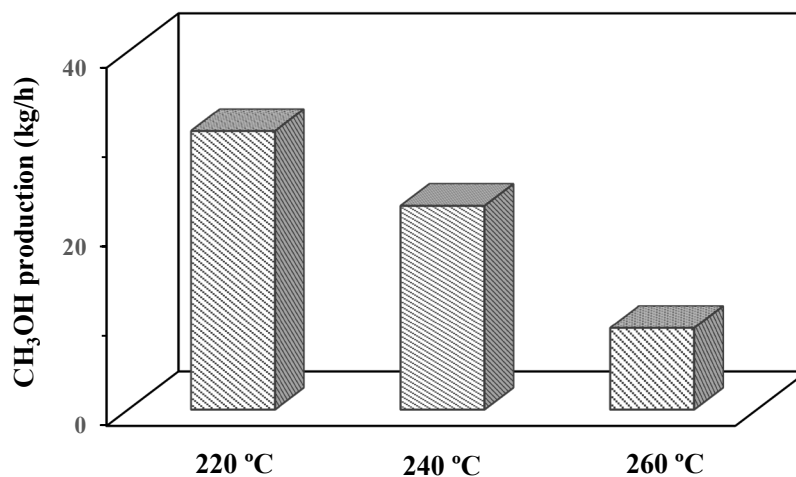


480

481 **Figure 9.** Pressure and temperature influence on CH<sub>3</sub>OH production

482

483 Once the pressure was fixed, the temperature was varied (220-260 °C). Figure 10  
484 shows the temperature effect on methanol production at 55 atm. As aforementioned,  
485 methanol production was highly favoured at low temperatures getting 32 kg/h at 220°C,  
486 whereas only 9 kg/h of methanol was obtained at the highest temperature. Therefore, the  
487 optimal conditions for methanol synthesis were fixed at 220 °C and 55 atm.



488

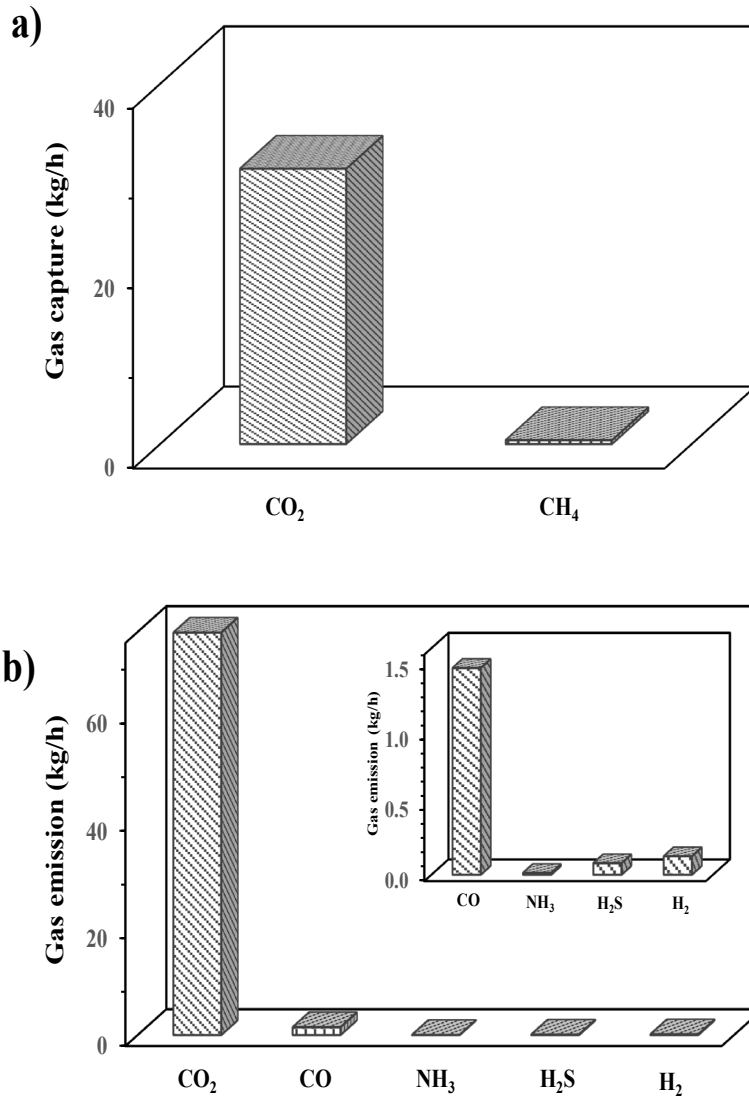
489 **Figure 10.** Temperature influence on methanol production (kg/h) at 55 atm.

490

491 3.3 Gas emission

492 The amount of greenhouse gases that the process was able to capture in the PSA  
 493 system, especially the amount of CO<sub>2</sub> and CH<sub>4</sub> and the other gas emissions was also  
 494 evaluated. Figure 11 shows the amount of CO<sub>2</sub> and CH<sub>4</sub> captured and gases released on  
 495 the whole process. The amount of CO<sub>2</sub> fed in the PSA system was 42 kg/h, being the  
 496 amount captured 32 kg/h. Almost 80% of all is sequestered. Although most of the carbon  
 497 dioxide produced in the gasification was captured, there was an amount of CO<sub>2</sub> released  
 498 from the combustion chamber (75 kg/h). Taking into account the amount of CO<sub>2</sub> produced  
 499 in the process, 30% was captured. According to the international energy outlook and  
 500 Sikarwar et al., [2, 25], by the year 2030, it will be adsorbed the 40% of the whole CO<sub>2</sub>  
 501 emissions. In the case of methane, 95% of total was captured in the fourth PSA unit.

502 Regarding the rest of the gases, NH<sub>3</sub> and H<sub>2</sub>S emissions were low, being associated  
 503 with the biomass selected in the present simulation which had low nitrogen and sulphur  
 504 content.



505

506

**Figure 11.** a) Gas capture (kg/h); b) Gas emission (kg/h)

### 507 3.4 Optimal process improvement

508 Once the simulation was validated, optimised and evaluated, an improvement of the  
 509 process was proposed. At this point, the waste stream of methanol synthesis, whose  
 510 composition was 70% of H<sub>2</sub> and 30% of the gases CO, CO<sub>2</sub> and CH<sub>4</sub>, was recirculated to  
 511 the combustion chamber in the gasification process. Figure 12 illustrates the comparison  
 512 between the results obtained before and after the recycle. It can be seen that the recycle  
 513 improved significantly the whole process yield.

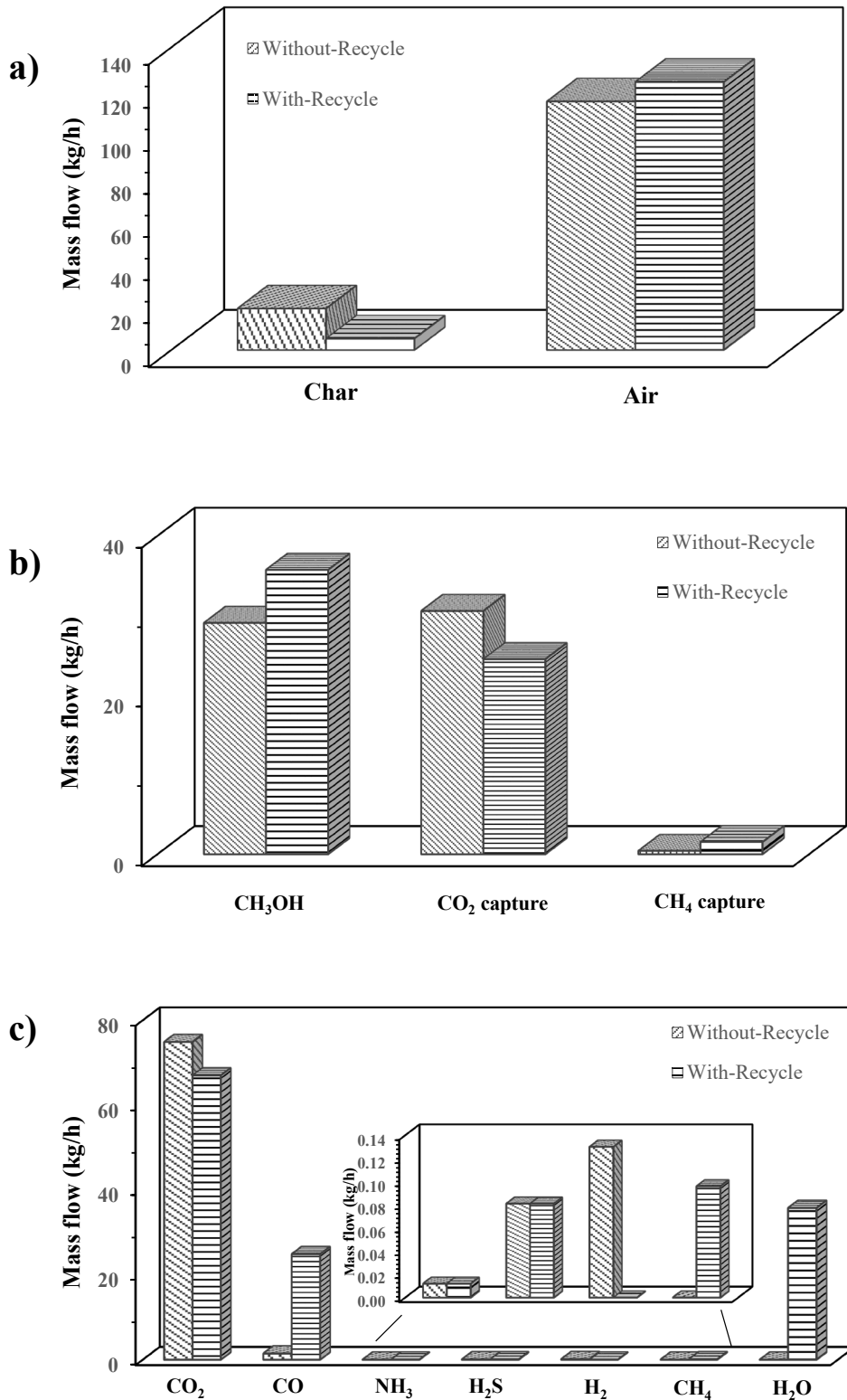
514        Regarding the combustion chamber of gasifier, before the recycle, it was necessary to  
515 separate about 40% of the char to achieve the gasification temperature, but with the  
516 increase of H<sub>2</sub> in the combustion process, it was just necessary to separate 10% of the  
517 char. This separation reduction implied that there was a higher amount of char available  
518 for the gasification process, favouring water gas and Boudouard reactions. In addition, it  
519 also increased the energy produced in the combustion process.

520        On the other hand, the air necessary in the combustion process slightly increased  
521 because the amount of gases to be burnt was higher. However, the increase of air needed  
522 was low in comparison with the decrease of the char needed in the combustion chamber.

523        As the carbon available for the gasification process was higher, the amount of CO  
524 produced increased, causing the improvement of methanol production. Furthermore, the  
525 increasing of CO concentration involved a decrease in the CO<sub>2</sub> production due to the  
526 gasification reactions. For this reason, it was observed that the CO<sub>2</sub> capture after the  
527 recycle was lower. In addition, the increase in carbon content also caused the higher CH<sub>4</sub>  
528 production explaining the enhancement in CH<sub>4</sub> capture.

529        Finally, in relation to the gas emission, the CO<sub>2</sub> emission decreased, being associated  
530 with the lower amount of char burnt in the combustion chamber and the higher amount  
531 of hydrogen involved. H<sub>2</sub> reacted with the oxygen to produce water preventing that all  
532 the oxygen reacted with the carbon to produce CO<sub>2</sub>. The recycle only modified the amount  
533 of carbon in the gasification process, thus, NH<sub>3</sub> and H<sub>2</sub>S emissions were kept due to  
534 sulphur and nitrogen content was not changed.





535

536 **Figure 12.** Comparison with and without-recycle for: a) char and air in the combustion

537 chamber; b) methanol production and GHG capture; c) gas emission.

538 **4 Conclusions**

539 In this work, a simulation of methanol synthesis from syngas obtained through pine  
540 biomass gasification using Aspen Plus<sup>®</sup> simulation software was developed. The next  
541 conclusions can be drawn:

542 - The gasification process was simulated using a thermodynamic equilibrium model  
543 which is based on the minimization of the Gibbs free energy of the system. A double  
544 chamber gasifier, which allows the separation of the gasification and combustion zones  
545 to obtain a high-quality gas, was considered. The influence of the steam to biomass (S/B)  
546 mass ratio and the temperature on the gas product composition and methanol production  
547 was studied. The best calculated operational condition of the process was 900°C and a  
548 S/B mass ratio of 0.9.

549 - One of the main technical barriers for the syngas production is the presence of tar  
550 coming from the gasification process. According to the simulation performed, tar  
551 production was hindered with increasing temperatures and steam flow rates. Dolomite  
552 was used as the catalyst in the decomposition of tar due to its low cost.

553 - A pressure swing adsorption (PSA) process was considered to clean the syngas  
554 and simultaneously capture the greenhouse gases. Therefore, about 80% of the CO<sub>2</sub> and  
555 95% of the CH<sub>4</sub> were sequestered.

556 - Once the H<sub>2</sub>/CO molar ratio of the clean syngas was fitted, the methanol synthesis  
557 proceeded. Although the methanol production is favoured at high pressures and low  
558 temperatures, a pressure of 55 atm was selected to avoid operational issues. Thus, 220°C  
559 and 55 atm were selected as the optimal operation conditions for the methanol synthesis.

560 - Finally, to improve the process yield, the methanol synthesis waste stream is  
561 recycled to the combustion chamber. With this recycle, the carbon required to burn is

562 reduced from 40 to 10%. Thus, there is a higher amount of carbon available to be used in  
563 the gasification process.

#### 564 **Acknowledgments**

565 Authors acknowledge the financial support from the Spanish government (Grant  
566 No. FPU15/02653).

#### 567 **References**

568 [1] O. Dessens, G. Anandarajah, A. Gambhir. Limiting global warming to 2 °C: What do  
569 the latest mitigation studies tell us about costs, technologies and other impacts? Energy  
570 Strategy Reviews. 13-14 (2016) 67-76.

571 [2] V.S. Sikarwar, M. Zhao, P.S. Fennell, N. Shah, E.J. Anthony. Progress in biofuel  
572 production from gasification. Progress in Energy and Combustion Science. 61 (2017)  
573 189-248.

574 [3] J.H. Pauls, N. Mahinpey, E. Mostafavi. Simulation of air-steam gasification of woody  
575 biomass in a bubbling fluidized bed using Aspen Plus: A comprehensive model including  
576 pyrolysis, hydrodynamics and tar production. Biomass and Bioenergy. 95 (2016) 157-66.

577 [4] L.P.R. Pala, Q. Wang, G. Kolb, V. Hessel. Steam gasification of biomass with  
578 subsequent syngas adjustment using shift reaction for syngas production: An Aspen Plus  
579 model. Renewable Energy. 101 (2017) 484-92.

580 [5] W.-X. Peng, S.-B. Ge, A.G. Ebadi, H. Hisoriev, M.J. Esfahani. Syngas production by  
581 catalytic co-gasification of coal-biomass blends in a circulating fluidized bed gasifier.  
582 Journal of Cleaner Production. 168 (2017) 1513-7.

583 [6] G. Guan, M. Kaewpanha, X. Hao, A. Abudula. Catalytic steam reforming of biomass  
584 tar: Prospects and challenges. Renewable and Sustainable Energy Reviews. 58 (2016)  
585 450-61.

- 586 [7] C. Berrueco, D. Montané, B. Matas Güell, G. del Alamo. Effect of temperature and  
587 dolomite on tar formation during gasification of torrefied biomass in a pressurized  
588 fluidized bed. *Energy*. 66 (2014) 849-59.
- 589 [8] J.F. González, S. Román, G. Engo, J.M. Encinar, G. Martínez. Reduction of tars by  
590 dolomite cracking during two-stage gasification of olive cake. *Biomass and Bioenergy*.  
591 35 (2011) 4324-30.
- 592 [9] F.J. Gutiérrez Ortiz, A. Serrera, S. Galera, P. Ollero. Methanol synthesis from syngas  
593 obtained by supercritical water reforming of glycerol. *Fuel*. 105 (2013) 739-51.
- 594 [10] N. Álvarez-Gutiérrez, M.V. Gil, F. Rubiera, C. Pevida. Kinetics of CO<sub>2</sub> adsorption  
595 on cherry stone-based carbons in CO<sub>2</sub>/CH<sub>4</sub> separations. *Chemical Engineering Journal*.  
596 307 (2017) 249-57.
- 597 [11] R. Krishnamurthy. Hydrogen and carbon monoxide production by hydrocarbon  
598 steam reforming and pressure swing adsorption purification. Google Patents1992.
- 599 [12] J.A. Batdorf. Method and apparatus for methanol and other fuel production. Google  
600 Patents2010.
- 601 [13] N.D. Couto, V.B. Silva, E. Monteiro, A. Rouboa. Assessment of municipal solid  
602 wastes gasification in a semi-industrial gasifier using syngas quality indices. *Energy*. 93  
603 (2015) 864-73.
- 604 [14] J.H. Pauls, N. Mahinpey, E. Mostafavi. Simulation of air-steam gasification of  
605 woody biomass in a bubbling fluidized bed using Aspen Plus: A comprehensive model  
606 including pyrolysis, hydrodynamics and tar production. *Biomass and Bioenergy*. 95  
607 (2016) 157-66.
- 608 [15] M. Zhai, L. Guo, Y. Wang, Y. Zhang, P. Dong, H. Jin. Process simulation of staging  
609 pyrolysis and steam gasification for pine sawdust. *International Journal of Hydrogen*  
610 *Energy*. 41 (2016) 21926-35.

- 611 [16] S. Nilsson, A. Gómez-Barea, D. Fuentes-Cano, P. Ollero. Gasification of biomass  
612 and waste in a staged fluidized bed gasifier: Modeling and comparison with one-stage  
613 units. *Fuel*. 97 (2012) 730-40.
- 614 [17] K. Im-orb, A. Arpornwichanop. Techno-environmental analysis of the biomass  
615 gasification and Fischer-Tropsch integrated process for the co-production of bio-fuel and  
616 power. *Energy*. 112 (2016) 121-32.
- 617 [18] M. Fernandez-Lopez, J. Pedroche, J.L. Valverde, L. Sanchez-Silva. Simulation of  
618 the gasification of animal wastes in a dual gasifier using Aspen Plus®. *Energy*  
619 *Conversion and Management*. 140 (2017) 211-7.
- 620 [19] L.P.R. Pala, Q. Wang, G. Kolb, V. Hessel. Steam gasification of biomass with  
621 subsequent syngas adjustment using shift reaction for syngas production: An Aspen Plus  
622 model. *Renewable Energy*. 101 (2017) 484-92.
- 623 [20] B. Hejazi, J.R. Grace, X. Bi, A. Mahecha-Botero. Kinetic Model of Steam  
624 Gasification of Biomass in a Dual Fluidized Bed Reactor: Comparison with Pilot-Plant  
625 Experimental Results. *Energy & Fuels*. 31 (2017) 12141-55.
- 626 [21] F.J. Gutiérrez Ortiz, A. Serrera, S. Galera, P. Ollero. Methanol synthesis from syngas  
627 obtained by supercritical water reforming of glycerol. *Fuel*. 105 (2013) 739-51.
- 628 [22] P. Trop, B. Anicic, D. Goricanec. Production of methanol from a mixture of torrefied  
629 biomass and coal. *Energy*. 77 (2014) 125-32.
- 630 [23] L. Shen, Y. Gao, J. Xiao. Simulation of hydrogen production from biomass  
631 gasification in interconnected fluidized beds. *Biomass and Bioenergy*. 32 (2008) 120-7.
- 632 [24] S. Luo, Y. Zhou, C. Yi. Syngas production by catalytic steam gasification of  
633 municipal solid waste in fixed-bed reactor. *Energy*. 44 (2012) 391-5.
- 634 [25] I.E. Outlook. DOE/IEA-0484. International Energy Outlook 2016, With Projections  
635 to 2040. 2016. p. [www.eia.gov/forecasts/ieo](http://www.eia.gov/forecasts/ieo).

636 **APPENDIX A**

637 **Table A1:** Design specification DS-1

<b>VARIABLE</b>	<b>DEFINITION</b>		
H <sub>2</sub>	Mole-flow Stream=45 Substream=MIXED Component=H <sub>2</sub> Units=kmol/h		
CO	Mole-flow Stream=45 Substream=MIXED Component=CO Units=kmol/h		
<b>ESPECIFICATION</b>		<b>MANIPULATED VARIABLE</b>	
Spec:	CO	Type:	Block-Var
Target:	H <sub>2</sub> /2.4	Block:	SPLIT-1
Tolerance:	0.01	Variable:	FLOW/FRAC
		Sentence:	FLOW/FRAC
Manipulated variable limits		ID1:	41
Lower:	0	ID2:	-
Upper:	1	ID3:	-

638

639 **Table A2:** Design specification DS-2

<b>VARIABLE</b>	<b>DEFINITION</b>		
CO <sub>2</sub>	Mole-flow Stream=45 Substream=MIXED Component=CO <sub>2</sub> Units=kmol/h		
CO	Mole-flow Stream=45 Substream=MIXED Component=CO Units=kmol/h		
<b>ESPECIFICATION</b>		<b>MANIPULATED VARIABLE</b>	
Spec:	CO <sub>2</sub>	Type:	Block-Var
Target:	0.13·CO	Block:	SPLIT-2
Tolerance:	0.01	Variable:	FLOW/FRAC
		Sentence:	FLOW/FRAC
Manipulated variable limits		ID1:	33
Lower:	0	ID2:	-
Upper:	1	ID3:	-

640

641

642

643

644

645

646

647

648

649 **Table A3:** Design specification DS-3

<b>VARIABLE</b>	<b>DEFINITION</b>		
FAIR	Mole-flow Stream=8 Substream=MIXED Component=O <sub>2</sub> Units=kmol/h		
FC	Mole-flow Stream=5 Substream=MIXED Component=C Units=kmol/h		
<b>ESPECIFICATION</b>		<b>MANIPULATED VARIABLE</b>	
Spec:	FAIR	Type:	Mole-flow
Target:	1.2·FC	Stream:	54
Tolerance:	0.01	Substream:	Mixed
		Component:	O <sub>2</sub>
Manipulated variable limits		Units:	Kmol/h
Lower:	1		
Upper:	1		

650

651 **Table A4:** Design specification DS-4

<b>VARIABLE</b>	<b>DEFINITION</b>		
TGASIF	Stream-Var Stream=11 Substream=MIXED Variable=TEMP Units=C		
<b>ESPECIFICATION</b>		<b>MANIPULATED VARIABLE</b>	
Spec:	TGASIF	Type:	Block-Var
Target:	800-900-1000 °C	Block:	SEP-1
Tolerance:	1	Variable:	FLOW/FAC
		Sentence:	FLOW/FAC
Manipulated variable limits		ID1:	CISOLID
Lower:	0,000001	ID2:	5
Upper:	0,999999	ID3:	C

652